Hindawi Publishing Corporation
International Journal of Spectroscopy
Volume 2010, Article ID 323848, 6 pages
doi:10.1155/2010/323848

Research Article

Temperature Dependences of the Quantum-Mechanical and Semi-Classical Spectral-Line Widths and the Separation n_0 of the Impact and Non-Impact Regions for an Ar-Perturbed/K-Radiator System

W. C. Kreye

Research and Instructional Computer Centre, Chemistry Department, Wright State University, Dayton, OH 45435, USA

Correspondence should be addressed to W. C. Kreye, warren.kreye@wright.edu

Received 20 May 2010; Accepted 3 September 2010

Academic Editor: David Ramaker

Quantum-mechanical and semi-classical spectral-line shapes are computed at $T = 400$, 800, and 1000 K for the line core of the 5802 Å line of the Ar-Perturbed/K-Radiator system. HWHMs (w's) are measured from computed full spectral-line shapes. The final-state pseudopotential is for the $7s^2S_{1/2}$ state, and the initial-state potential is for the $4p^2P_{3/2,3/2}$ state. Three high-pressure (P) log(w)—versus—log(P) curves, corresponding to the non-impact region, intersect a similar set of low-P, impact-region curves at intersections, P_0's. Similarly, for two sets of log(w)—versus—log(n) curves, which yield intersections, n_0's, where n is the perturber density. These n_0's and p_0's separate the two regions and represent the upper limits of the impact regions. A specific validity condition for the impact region is given by the equation $n \leq n_0$. From an earlier spectroscopic, Fabry-Perot paper, $w_{\text{expt}} = 0.021\,\text{cm}^{-1}$ at $T = 400$ K and $P = 10$ torr. Two theoretical values, $w_{\text{theor}} = 0.025$ and $0.062\,\text{cm}^{-1}$ corresponding to two different pseudo-potentials, are reported. Two T-dependent figures are given, in which the first shows an increase in the impact region with T, based on P as the basic parameter, and the second which shows a decrease in the impact region with T, based on n as the basic parameter.

1. Introduction

Spectral-line-shape and line-broadening studies have been performed for many years, as evidenced by the 30-year, 15-plus volumes of the AIP "Spectral Line Shapes", typically, Back [1]. However, there are four areas that still have to be addressed in detail:

(1) the effects of temperature (T) upon the HWHM (w) of the spectral line and upon the perturber-density separation n_0 between the impact and non-impact regions;

(2) the acquisition of specific limits of the validity conditions for the impact approximation—Baranger [2] reported that it is "a subject which has been very neglected;"

(3) the variation of the extent (size) of the impact (approximation) region with T—a controversy exists as to whether the region increases or decreases with T;

(4) a partial testing of the validity of the present theoretical development and programming—this will be achieved by comparing present computed values of w with previous Fabry-Perot spectroscopic measurements; see the work of Kreye in [3].

This study is a continuation of the work by Kreye [4] on the 5802 Å spectral line of the K/Ar system at 400 K. Quantum-mechanical (QM) and semi-classical (SC) theories were used to compute full spectral-line shapes, from which the values of w and the shift (d) were measured; a realistic pseudo-potential for the initial state, $4p^2P_{3/2,1/2}$, was used as the basis for his computations; A measured P_0, was employed as the separation of the impact region from the non-impact region and linear log(w)—versus—log(P)

curves were introduced to show the dependence of w upon P.

This paper computes the effects of T upon w and P_0, introduces the the perturber density n, and uses the pseudopotential, $7s^2S_{1/2}$, to represent the final state and a pseudopotential to represent the initial state. (This system was chosen because of its familiarity to the author, but the theory and programs are sufficiently general for other rare-gas/alkali systems.) The temperatures studied are 400, 800, and 1000 K, and the pressures range from 10^3 to 10^6 torr.

The following papers are pertinent to the present study: the review paper by Allard and Kielkopf [5], which contains the SC theory used in this study and describes the pseudopotentials; the paper of Baranger [2] in which he derives the QM impact approximation theory, the non-impact-region theory and considers in detail transitions between two states; the previously mentioned paper by Kreye [4] in which the theoretical expressions of Baranger [2] are expanded into computable form; the paper of Szudy and Baylis [6] in which the unified theory of line broadening is developed; the experimental/theoretical works of Kreye and Kielkopf [7–9]; the T-dependent measurements by Vaughan [10] of the Kr/rare-gas systems at 89 and 295 K; the work of Baylis [11] who expands the pseudopotential theory.

2. Theory

Much of the theory is presented in [4], and a brief summary is included here. As in [4], the basic computations are performed with the autocorrelation function $\Phi(s)$ rather than with the line-shape expression $F(\omega)$. In the above, $\Phi(s) = \phi(s)^N$, where N is the number of perturbers and where $\phi(s)$ is the auto-correlation function for a single perturber. The general $g(s)$-type function is shown to enter in as

$$\Phi(s) = \exp[-ng(s)], \tag{1}$$

where n is the perturber density. The various QM and SC forms of $g(s)$ are presented below. The expression for the line shape $F(\omega)$ is taken from [2, equation (6)], and it is renumbered here as

$$F(\omega) = \frac{1}{2\pi} \cdot 2 \cdot \int_0^{s_{\max}} ds \cdot \exp\{-n \cdot \Re[g(s)]\} \times \cos\{-n \cdot \Im[g(s)] + \omega s\}. \tag{2}$$

The SC expression for $g_{\mathrm{NI}}(s)$ and $g_{\mathrm{I}}(s)$ are given in [5]: equation (55) is for the non-impact (NI) region, and equations (56, 57) are for the impact (I) region. The corresponding expressions for the $\Re[g_{\mathrm{NI}}(s)]$, $\Im[g_{\mathrm{NI}}(s)]$, and the impact terms can be put into (2) for $F(\omega)$.

The QM expression for $g_1(s)$ in the impact region is obtained from Baranger's [2, equation (31)]; it becomes, after rearranging and modifying,

$$g_1(s) = is\left\langle \psi_{fk}^* | \triangle V | \vec{k} \right\rangle. \tag{3}$$

The QM expression for $g(s)$ in the non-impact region is given by Baranger's equation (29), and after rearranging and modifying, it becomes

$$g(s) = is\left\langle \psi_{fk}^* | \triangle V | \vec{k} \right\rangle + \int \frac{d^3\vec{k'}}{8\pi^3} \left| \left\langle \psi_{fk'}^* | \triangle V | \vec{k} \right\rangle \right|^2 \frac{1 - e^{-i(\epsilon - \epsilon')s}}{(\epsilon - \epsilon')(\epsilon - \epsilon' - i\eta)}, \tag{4}$$

where $\vec{k} = \exp(-i\vec{k} \cdot \vec{r'})$ and $\triangle V = 7s^2S_{1/2} - 4p^2P_{3/2,3/2}$.

In (4), $\psi_{fk'}^*$ is the final-state wave function for the introduced set of $\vec{k'}$ states, and η is an infinitesimal. This equation holds for the complete range of s and consists of two parts: the first term on the right is identical with (3) in the present paper, and it corresponds to the impact region with "large" s and small P. The second term corresponds to the remaining "small" s and large P; therefore it holds for the non-impact region. This second term is defined as $g_2(s)$ and is based on [4, equation (11)]. Our treating (4) as a sum of a small-s part and a large-s part is reminiscent of the 1956 unpublished work of Anderson and Talman [5, page 1134], who separated the auto-correlation function into two parts: one for small s, one for large s.

The terms in (3), (4): ψ_{fk}^*, $\psi_{fk'}^*$, and $\vec{k}$ are expanded as sums of partial waves. $\vec{k}$ is given by [4, equation (13)]. Also,

$$\psi_{fk'}^* = \sum_{l=0}^{l=l_{\max}} (2l+1)\left(-i^l\right) \exp\left(-i\delta_{f,l}\right) R_{f,l}[k'(\epsilon')r'] P_l(\cos\Theta). \tag{5}$$

The expression for ψ_{fk}^* can be obtained from $\psi_{fk'}^*$. In these equations, l is the angular momentum quantum number, P_l is the Legendre polynomial, $R_{f,l}$ is the radial wave function, and $\delta_{f,l}$ is the phase shift for the final state. The parameters are defined as: $\epsilon = 3k_BT/2\hbar$, $k'(\epsilon') = \sqrt{(2\mu\epsilon'/\hbar)}$, $k = \sqrt{(3\mu k_BT/\hbar^2)}$, and $v = \sqrt{(3k_BT/\mu)}$. ϵ' is the independent variable. The above v is the root mean square velocity which replaces the need for Maxwell/Boltzmann distribution of velocities.

In order to compute the phase shift $\delta_{f,l}$ and the radial wave function $R_{f,l}[k'(\epsilon')(r')]$, the Schroedinger equation is expressed in terms of the dimensionless variable, $\rho = kr'$ instead of r'. Therefore, we obtain the following form of the Schroedinger equation for the final state:

$$\frac{d^2R_{f,l}}{d\rho^2} + \frac{2dR_{f,l}}{\rho d\rho} + \left[1 - 4\mu\pi\frac{\left(V_f(\rho)\right)c}{(\hbar k^2)} - \frac{l(l+1)}{\rho^2}\right] R_{f,l} = 0, \tag{6}$$

where μ is the reduced mass.

In order to integrate (6) from the initial point $a_1 = 5.0$ Å to the final point $a_2 = 20.0$ Å, the initial conditions (IC's) at a_1 are needed. The approximate IC's for equation (31) are

$$R_{f,l}(ka_1) = j_l(ka_1), \qquad R'_{f,l}(ka_1) = j_l'(ka_1), \tag{7}$$

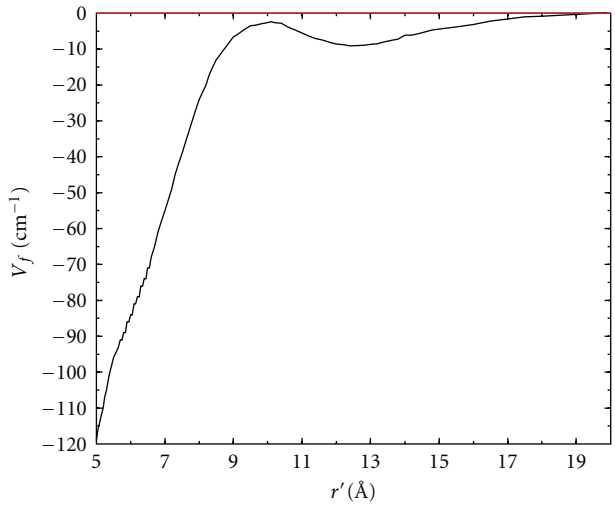

FIGURE 1: A plot of V_f—versus—r', where V_f correponds to the electronic state, $7s^2S_{1/2}$. The pseudopotential was formulated by Allard and Kielkopf in [5].

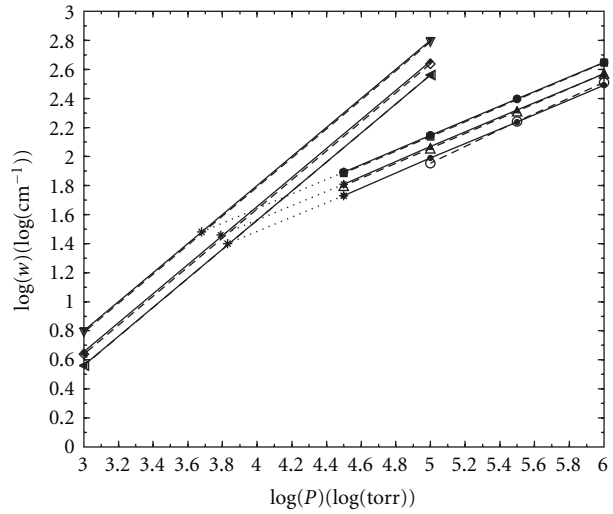

FIGURE 2: Plots of log(w)—versus—log(P) in the two pressure regions: The high-P, non-impact region ($10^{4.5}$ to 10^6 torr); and the low-P, impact region (10^3 to 10^5 torr). Three sets of curves are presented at (counting down) 400, 800, and 1000 K. The QM curves are solid lines, and the SC curves are dashed lines in both regions. The dotted lines are approximate extrapolations from the QM non-impact curves. The intersection of an extrapolation with the corresponding QM impact-region curve, represented by an $*$, gives rise to P_0, the approximate separation between the impact and the non-impact regions.

where $j_l(ka_1)$ is the spherical Bessel function. The expression for the phase shift $\delta_{f,l}$ in terms of $R_{f,l}$ and $R'_{f,l}$ is based on, for example, Schiff [12, equation (19.14)], and the phase shift is computed at $r' = 20.0$ Å. The equations for $\Re[g_1(s)]$ and $\Re[g_2(s)]$ are found in [4, equations (17, 18)]. Similarly for the imaginary terms. All these terms can be substituted into (2) to give the QM $F(\omega)$'s.

3. Computational and Analytic Details

Several of the analytic details in the present study are the same as those in [4], such as: the use of linear log(w)—versus—log(P) curves, the numerical computation of the three-angle integration term in the expanded (4), the integration over ϵ', and the integration over s.

Additional analytic details are:

(1) the pseudo-potential was expanded into 27500 elements using a spline technique;

(2) the integration of (6) used a second-degree Runge-Kutta method;

(3) in order to determine $l_{\max}$, we found for the present paper that it was impossible to use the method of [4], which consisted of letting l increase until it leveled off at $l_{\max}$. The reason is that l does not level off to an asymptotic value, as can be shown. Therefore, the following methods were used to determine $l_{\max}$: in the impact region, $l_{\max}$ was set equal to 101, 108, and 121 for the corresponding values of $T = 400, 800$, and 1000 K. These were chosen so that $w_{\mathrm{QM}} \approx w_{\mathrm{SC}}$. In the non-impact region, $l_{\max}$ was set equal to 107, 153, and 171. These values were chosen to yield $w_{\mathrm{QM}} \approx w_{\mathrm{SC}}$. Moreover, it can be shown that these last choices have a theoretical basis which is based on Schiff's [12] equation, $l_{\max} = ka$, where a is defined as an "assumed radius beyond which the potential $U(r)$ is negligible". From Schiff's theoretical equation, $l_{\max} = 100, 140$, and 157. These theoretical "Schiff" values are within about 8% of our chosen values, 107, 153, and 171.

4. Results

4.1. Discussion of V_f—Figure 1 Depicts V_f-versus-r'.

4.2. Variation of log(w) *with* log(P) *and* log(w) *with* log(n). Figure 2 shows three lower log(w)—versus—log(P) curves in the impact (low-P) region for 400, 800, and 1000 K (reading down). The curves are linear with slopes, $d\ \log(w)/d\ \log(P)$, of 1.0, and there is good agreement between the SC and the QM curves. Figure 2 also shows three similar curves in the non-impact (high-P) region. The curves are linear with an average slope of 0.506 ± 0.001.

In Figure 2, the dotted lines are extrapolations from the non-impact-region QM curves, and they intersect the corresponding impact-region QM curves at points with $*$ markings. These intersections are defined as P_0's, and they represent, as introduced in [4], the approximate upper limits to the impact regions and the lower limits to the non-impact regions. Rigorously, the connections between the two regions would be represented by smooth, continuous-derivative curves. There is, at present, no quantitative theory for representing such smoothed curves.

Figure 3 shows a similar set of log(w)—versus—log(n) curves. Only the QM curves are shown. As in Figure 2, the impact-region curves have a slope of 1.0 and the non-impact-region curves have a slope of 0.507. (An interesting

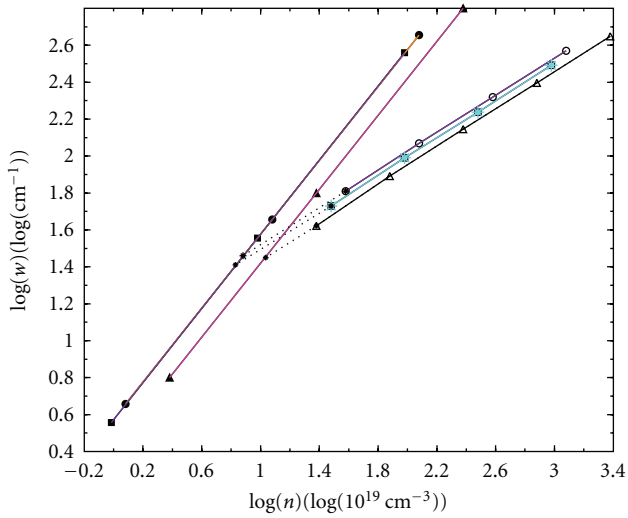

Figure 3: This plot shows a set of three QM log(w)—versus—log(n) curves in the non-impact region (large n) at temperatures: T = 400 K (empty circles), T = 800 K (empty squares), and T = 1000 K (empty triangles). A similar set appears in the impact region (small n): T = 400 K (filled circles), T = 800 K (filled squares), and T = 1000 K (filled triangles). The dotted lines are extrapolations from the non-impact-region QM curves; and they intersect the corresponding impact-region curves at n_0's.

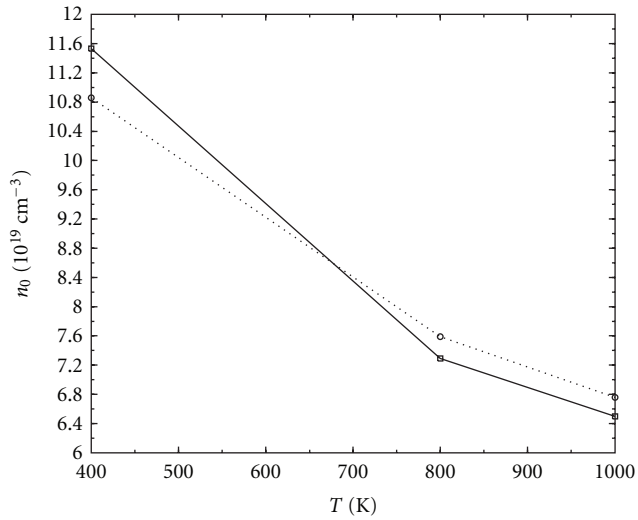

Figure 4: Two plots of n_0—versus—T are shown in this plot. The data for the solid curve are taken from the intersections P_0's in Figure 2 (log(w)—versus—log(P)), and n_0 is calculated from $n_0 = P_0/RT$. The data for the dotted curve is taken directly from the n_0 intersections in Figure 3. The curves do not exactly overlap because of the uncertainties in the two sets of the extrapolations in Figures 2 and 3. These curves establish that the impact region, defined by n_0, decreases with T when n is the basic parameter.

comment is found in [5, page 1148], which confirms the above slope, because equation (296) in that reference predicts that "the width (HWHM) of the line grows only as $n^{1/2}$"). The extrapolations of the non-impact curves with the impact curves intersect at $*$'s, and these points are designated as n_0's. These n_0's are defined as the P_0's are defined.

4.3. Temperature Dependences of n_0 and P_0. Figure 4 shows the curves for n_0—versus—T. The solid curve corresponds to n_0 data obtained directly from the intersections of the curves in Figure 3. The n_0 data for the dotted curve in Figure 4 are obtained from the P_0 intersections in Figure 2, where $n_0 = P_0/RT$. Both show an initial decrease of n_0 with increasing T, followed by a gradual leveling off. Thus, the extent or size of the impact region, n_0, *decreases* with increasing T, when the perturber density n is the basic parameter.

On the other hand, Figure 5, which exhibits the variation of P_0 with T, indicates that P_0 *increases* with increasing T, when P is the basic parameter. In other words, the extent of the impact region increases with T. Although n is the more significant parameter in line-broadening studies, (e.g., in (2), n appears in the exponent and in the cos factors.), P is a more important parameter from an experimental point of view. An advantage of this increase in the impact region at higher temperatures is that one can use the simpler impact-region theory to extract such results as a predicted T from a measured w and P.

The controversy mentioned in part (3) in the Introduction as to whether the impact region increases or decreases with T is herein clarified: the extent of the impact region both increases and decreases with T, depending upon whether P or n is the basic parameter.

4.4. Validity Conditions for the Impact (Approximation) Region. Baranger [2, page 482], states that the validity condition for the impact approximation is "a subject which has been very neglected." We tackle these validity conditions with two approaches:

(1) in the the first approach, we use the theoretical treatment of Baranger [2, pages 489–492], and we present it here extremely briefly: in his first method, he introduces the collision time τ; and the qualitative validity condition is that the following relation must be satisfied: $s \ll \tau$. In his second method, he requires that the difference between the real part of the *exact* $g(s)$, in his equation (29), and the *impact approximation* $g(s)$, in his equation (31), must be smaller than either of them in order for the impact approximation to be valid. This condition requires that the following relation must hold: $4\int d^3k'/(8\pi^3)[|\langle\vec{k'}|V|\psi\rangle| - |\langle\vec{k''}|V|'\psi\rangle|/(\epsilon - \epsilon')]^2 \ll n^{-1}$, where n^{-1} is the volume of a perturber. In his last method, he introduces a "collision volume", U, which is defined as the volume in which the wave function propagates differently from the wave function with energy ϵ. The corresponding validity condition is that U must satisfy the relation: $U \ll n^{-1}$;

(2) in the second approach, we use the results of the present study. We obtain a more specific validity condition than Baranger's validity conditions, all of which involve the less-than, less-than $\ll$ relation. Our study yields a specific, limit-type validity condition, namely, numbers, n_0 and P_0, which are defined

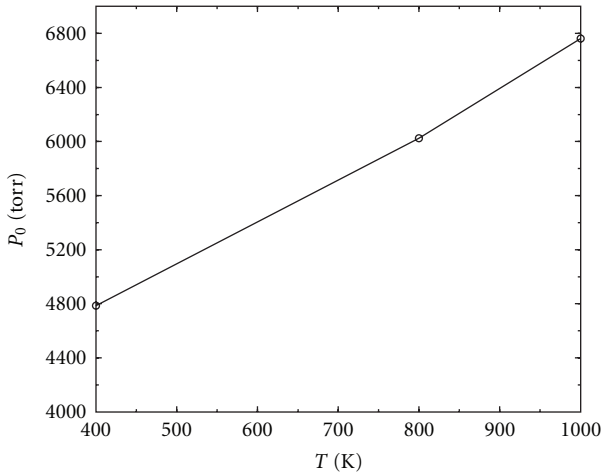

FIGURE 5: This plot shows the P_0—versus—T curve, where the P_0 intersections are taken from Figure 2. This curve establishes that the impact region, defined by P_0, increases with increasing T when P is the basic parameter.

as the upper limits to the impact region when T and the particular system are given. Thus, the validity conditions for the impact region are

$$n \leq n_0, \qquad P \leq P_0. \tag{8}$$

To summarize, there are two types of validity conditions: the first is based on a $\ll$ condition and the second on a $\leq$ condition. We believe that the second $\leq$ condition is of greater practicable value since the question would arise, with the $\ll$ condition, whether a given n is small *enough* to satisfy the $\ll$ condition. The question does not arise for the $\leq$ condition.

4.5. Comparison of Experimental with Theoretical Results. The value of an experimental slope, $\text{slope}_{\text{expt}} \equiv d\log(w)/d\log(P)$, is obtained from Figure 3 in the Fabry-Perot paper [3]. The curve is in the impact region. Between $\approx$3.2 and $\approx$11.3 torr, the value of $\text{slope}_{\text{expt}}$ can be calculated as $0.94 \pm 10\%$. A theoretical slope is obtained from Figure 2 in the present paper. In the impact region, $\text{slope}_{\text{theor}} = 1.00$. Thus, there is agreement between the two slopes.

An experimental, w_{expt}, is obtained from [3], Figure 3. That paper shows that the instrumentally corrected $w_{\text{expt}} = 0.021\,\text{cm}^{-1}$, at $T = 400\,\text{K}$ and $P = 10\,\text{torr}$. One theoretical value, w_{theor}, is taken from [4]: from Figure 3 in that reference, $w_{\text{theor}} = 0.025\,\text{cm}^{-1}$. A second w_{theor} is from the present study. Under the same conditions, $w_{\text{theor}} = 0.062\,\text{cm}^{-1}$.

The near agreement between the above $w_{\text{expt}} = 0.021\,\text{cm}^{-1}$ and $w_{\text{theor}} = 0.025\,\text{cm}^{-1}$ partially establishes the validity of the theory and programming in the present study.

5. Conclusions

(1) The separation between the impact and non-impact regions can be represented by the intersection, n_0 or P_0, of a non-impact-region (extended) curve, $\log(w)$—versus—$\log(n)$, or a similar $\log(w)$—versus—$\log(P)$ curve, with the corresponding impact-region curve.

(2) An n_0—versus—T curve shows that the upper limit, n_0, of the impact region decreases with T whereas in a P_0—versus—T curve, the upper limit, P_0, increases with T.

(3) A specific limit to the validity condition for the impact region has been defined as, $n \leq n_0$, in contrast to Baranger's conditions which use the general $\ll$ term.

(4) The near agreement between $w_{\text{expt}} = 0.021\,\text{cm}^{-1}$ and $w_{\text{theor}} = 0.025\,\text{cm}^{-1}$ partially establishes the validity of the theory and the programming in the present study. Thus, this program can be used for other rare-gas/alkali studies.

Acknowledgments

W. C. Kreye acknowledges the continued support of Professor John Kielkopf of the University of Louisville who also freely made available to me his excellent pseudo-potential programs. The author also acknowledges the support of the director and staff of CaTS at Wright State University and especially the manuscript preparatory help of Jeffery Jones, John Meyers, and Steve Wynne.

References

[1] C. A Back, "Spectral line shapes," in *Proceedings of the International Conference on Spectral Line Shapes*, vol. 645 of *AIP Conference Proceedings*, pp. 523–525, New York, NY, USA, 2002.

[2] M. Baranger, "Simplified quantum-mechanical theory of pressure broadening," *Physical Review*, vol. 111, no. 2, pp. 481–493, 1958.

[3] W. C. Kreye, "Temperature dependence of the shift, width and asymmetry of the potassium (4p-7s) 5802 $^\circ A$ line perturbed by argon," *Journal of Physics B: Atomic and Molecular Physics*, vol. 15, no. 3, article 020, pp. 371–386, 1982.

[4] W. C. Kreye, "Quantum-mechanical vs. semi-classical spectral-line widths and shifts from the line core in the non-impact region for the Ar-perturbed/ K-radiator system," *Journal of Quantitative Spectroscopy and Radiative Transfer*, vol. 107, no. 1, pp. 154–163, 2007.

[5] N. Allard and J. Kielkopf, "The effect of neutral nonresonant collisions on atomic spectral lines," *Reviews of Modern Physics*, vol. 54, no. 4, pp. 1103–1182, 1982.

[6] J. Szudy and W. E. Baylis, "Profiles of line wings and rainbow satellites associated with optical and radiative collisions," *Physics Report*, vol. 266, no. 3-4, pp. 127–227, 1996.

[7] W. C. Kreye and J. F. Kielkopf, "Temperature dependence of spectral line shifts in pressure broadening," *Journal of Physics B: Atomic, Molecular and Optical*, vol. 24, pp. 65–76, 1991.

[8] W. C. Kreye and J. F. Kielkopf, "Non-adiabatic effects in the broadening and shift of the K 7s-4p transition by Ar," *Journal of Physics B: Atomic, Molecular and Optical Physics*, vol. 30, no. 9, pp. 2075–2091, 1997.

[9] W. C. Kreye and J. F. Kielkopf, "Evaluation of a quantum theory for the width and shift of an Ar-perturbed K-emission line in the non-impact region I.Morse potentials," in *Proceedings of the 16th Conference on Spectral Line Shapes*, vol. 12, pp. 325–326, 2002.

[10] J. M. Vaughan and Geoffrey Smith, "Interpretation of foreign-gas broadening and shift in krypton," *Physical Review*, vol. 166, no. 1, pp. 17–21, 1968.

[11] W. E. Baylis, "Semiempirical, pseudopotential calculation of alkali-noble-gas interatomic potentials," *The Journal of Chemical Physics*, vol. 51, no. 6, pp. 2665–2679, 1969.

[12] L. Schiff, *Quantum Mechanics*, McGraw-Hill, New York, NY, USA, 1949.